Focussing options using compound refractive lenses at beamline P10 of PETRA III

Journal of Physics: Conference Series **3010** (2025) 012059 doi:10.1088/1742-6596/3010/1/012059

Focussing options using compound refractive lenses at beamline P10 of PETRA III

Fabian Westermeier[1], Nimmi Das Anthuparambil[1,2], Zhe Ren[3], Wojciech Roseker[1], Rustam Rysov[4], Daniel Weschke[1], Han Xu[3] and Michael Sprung[1]

[1]Deutsches Elektronen-Synchrotron DESY, Notkestr. 85, 22607 Hamburg, Germany
[2]Department Physik, Universität Siegen, Walter-Flex-Straße 3, 57072 Siegen, Germany
[3]Institute of High Energy Physics, Chinese Academy of Sciences, Beijing, China
[4]European X-ray Free Electron Laser Facility, Holzkoppel 4, 22869 Schenefeld, Germany

E-mail: fabian.westermeier@desy.de

Abstract. In a coherent scattering experiment, one of the important experimental parameters is the speckle visibility, which can be changed by adjusting the size of the X-ray beam on the sample. Focussing optics provide therefore a convenient tool to increase the speckle visibility, while simultaneously increasing the flux density and thus the dose on the sample. At the Coherence Applications Beamline P10 different focussing options are used to optimize this interplay of dose and speckle visibility for a given experiment. Using compound refractive lenses, three different realizations are presented using a lens-to-sample distance of 0.45, 1.6 and 10.8 m. The resulting focal spot sizes range from around 1 μm $\times$ 1 μm to around 15 μm $\times$ 7 μm (horizontal $\times$ vertical direction).

1 Introduction

In a coherent scattering experiment, the scattered intensity is modulated due to interference effects, leading to a so called speckle pattern. One of the key quantities in a coherent scattering experiments is the visibility of these speckles, a quantity which is often termed the speckle contrast. While one key quantity influencing the speckle contrast is the degree of coherence of the X-rays impinging on the sample, another aspect is the setup employed and the experimental geometry. Here, three geometrical aspects define primarily the speckle visibility in a coherent scattering experiment: a) The sample to detector distance, where a larger distance allows the speckle pattern to expand further and thus increase the speckle visibility, b) the pixel size of the detector, where a larger pixel size can lead to a reduced speckle visibility, and c) the beam-size on the sample. The latter scales inversely with the speckle visibility for samples that are larger than the beam-size, i.e. a decreasing beam-size leads to a higher speckle visibility in a given setup. While both sample to detector distance and detector pixel size are usually fixed during an experiment, the beam-size on the sample can be changed relatively easily during an experiment and is thus the parameter which allows to tune the speckle visibility.

The usage of focussing optics is one method to change the beam-size, and thus the speckle visibility in a coherent scattering experiment, with the downside of leading to a higher photon flux density and thus radiation dose of the sample with a more focussed beam. This leads to the need to optimize the beam-size for a given experiment, to achieve an acceptable speckle visibility while reducing beam induced changes to the sample system under investigation. In the following, we will present three different focussing options realized at the Coherence Application Beamline P10 at PETRA III using compound refractive lenses (CRLs) [1, 2].

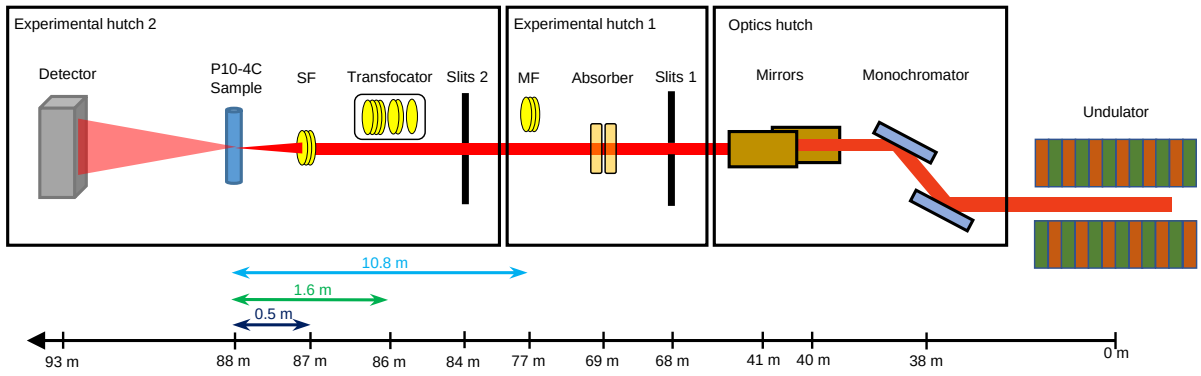

Figure 1: Schematic view of beamline P10. The arrow on the bottom indicates the distance of the displayed components from the source. The lens to sample distances of the medium focus (MF), transfocator and short focus (SF) are shown in light blue, green and dark blue, respectively.

2 Coherence Applications Beamline P10

The Coherence Application Beamline P10 at PETRA III is dedicated to perform coherent scattering experiments. It operates in a photon energy range of 5-16 keV using a Si(111) channel-cut monochromator. The main scientific drivers of the beamline are the investigation of structure and dynamics on nanometer to atomic length scales with X-ray photon correlation spectroscopy (XPCS) and X-ray Cross Correlation Analysis (XCCA) [3, 4], Bragg coherent diffraction imaging [5], 3D coherent diffraction imaging [6] and holographic imaging [7, 8]. The beamline operates four setups in two 12 m long experimental hutches. All setups are optimized to operate with specialized beam shaping and conditioning options. In the majority of cases the beamline lets the beam propagate as far as possible from the source to ease the spatial coherence filtering via slits before applying the specialized focusing optic of the selected setup. One of the setups is a multi-purpose XPCS setup (P10-4C) situated in the second experimental hutch of beamline P10, at a distance of 87.7 m from the source. It is based on a 4-circle Huber diffractometer in horizontal scattering geometry. The setup can reach scattering angles from 0-30° in combination with a 5 m long, rotatable flight path. By using a shorter flight path of approximately 2 m, the scattering angle range can be increased to 0-45°, making it feasible to reach the first maximum of the static structure factor peak for a number of hard condensed matter systems within the photon energy range of P10. While the sample area can be customized to allow for specific setups, in the standard configuration the sample is typically mounted on specialized inserts and placed inside a DN100 vacuum cube. This allows for a background-reduced, windowless operation.

2.1 Focusing options at the P10-4C setup

This highly versatile setup is usually used in combination with either an unfocused beam or three different focussing options based on CRLs:

- (a) short focus (SF) option, located 450 mm upstream of the sample,
- (b) transfocator (TF) option, located 1580 (± 150) mm upstream of the sample,
- (c) medium focus (MF) option, located 10800 mm upstream of the sample.

A schematic view of the beamline, displaying the position of the three different focussing options, is shown in figure 1. All three options feature two translational degrees of freedom, i.e. a horizontal and a vertical translation perpendicular to the beam direction, as well as the two rotational motions around these two axes to align and center the CRLs in the X-ray path. Option (b), the transfocator [9], offers two experimental possibilities not available for the short or medium focus. On the one hand the transfocator allows to change it's position by ± 150 mm along the beam direction, making it possible to adjust the focal spot to the sample position. On the other hand, it offers the possibility to choose between combinations of 12 different lens stacks (four 1D lens stacks and eight 2D lens stacks, the details can be found in reference [9]). In combination with the adjustable lens-to-sample distance it is enabling full coverage of

Table 1: Possible photon energies for the short focus (SF) and medium focus (MF) configuration for an energy range in between 5 - 16 keV. For the SF option, the number of Beryllium lenses with a radius of curvature of 50 μm are shown, while for the MF option, the number of Beryllium lenses with a radius of curvature of 500 μm are displayed.

SF N for R = 50μm	SF energy [keV]	MF N for R = 500μm	MF energy [keV]
5	5.51	2	5.01
7	6.52	4	7.19
9	7.41	6	8.80
11	8.20	8	10.16
13	8.92	10	11.36
15	9.59	12	12.44
17	10.22	14	13.44
		16	14.37
		18	15.24

the standard energy range of beamline P10 from 5 to 16 keV. The two other options do not offer this possibility. Both, the short and the medium focus, are installed at a fixed lens-to-sample distance. Both options can be equipped with a static number of 2D lenses of rotationally parabolic shape made out of Beryllium. At beamline P10 Beryllium refractive X-ray lens radii of curvature of 50, 100, 200, 500 and 1000 μm are available and can be installed. As the focal point of a particular lens stack depends both on the X-ray photon energy and the combination of lenses, the working energy for a particular experiment is restricted by the potential combinations of 2D lenses installed at either the SF or the MF. An overview of number possible lens combinations and corresponding photon energies in between the energy range of P10 from 5-16 keV is given in table 1. Please note that the available space for the installation of 2D lenses is limited to a maximum number of 18 individual lenses at both the SF and the MF. Here the MF, due to the larger focal distance with respect to the SF, can cover the full photon energy range of P10, while the energy range of the short focus option is limited to 5 - 10.5 keV.

For compound refractive lenses, in the thin film approximation, the focal length f shifts to smaller values with decreasing radius of curvature R, given by [10] $f = R/(2\delta)$ where δ is the refractive decrement. It is therefore possible to reach energies in between the ones listed in table 1 by combining the given lens combinations with lenses of larger radii of curvature.

2.2 Beam-sizes and speckle visibility

To quantify the beam-size for an experimental configuration, a knife edge - typically a thin gold or tungsten wire - is placed at the sample position and scanned through the X-ray beam. The transmitted intensity is recorded, and its derivative is fitted with a Gaussian function. The scans, derivatives and Gaussian fits for the short focus, transfocator and medium focus are shown in figure 2. The resulting beam-sizes in the horizontal and vertical direction are 1.0 μm $\times$ 0.7 μm for the SF, 3.2 μm $\times$ 2.4 μm for the TF and 15.6 μm $\times$ 7.6 μm for the MF.

Given the photon source size of beamline P10 with a vertical source size of $G_v = 14.1$ μm and a horizontal source size of $G_h = 84.6$ μm and correcting for the finite size of the X-ray beam in front of the CRLs which is smaller than the geometrical aperture of the lenses [11], the theoretical beam-sizes in the horizontal and vertical direction are 0.8 μm $\times$ 0.7 μm for the SF, 2.6 μm $\times$ 2.2 μm for the TF and 18.9 μm $\times$ 12.6 μm for the MF. This is, apart from the vertical beam-size of the MF, which was measured to be smaller than calculated, in good agreement with the obtained results.

One possibility to vary the beam-size on the sample is to move the sample slightly out of focus. Another option is given by the possibility to change the beam-size impinging on the CRLs. When the beam-size is smaller than the geometrical aperture of the CRLs, the diffraction limited focal spot changes as a function of beam-size that is collected by the CRLs [12]. The size of the X-ray beam which is subsequently focussed by the CRLs is defined by slits upstream of the lenses. Figure 3 displays the effect of the size of the beam defining aperture on the resulting beam-size for the medium focus option. Here, slit 1 in figure 1 has been used to define the beam-size. As displayed in figure 3(a) and (b), the focal spot size changes as a function of the size of the beam defining aperture in the same direction, i.e. the vertical

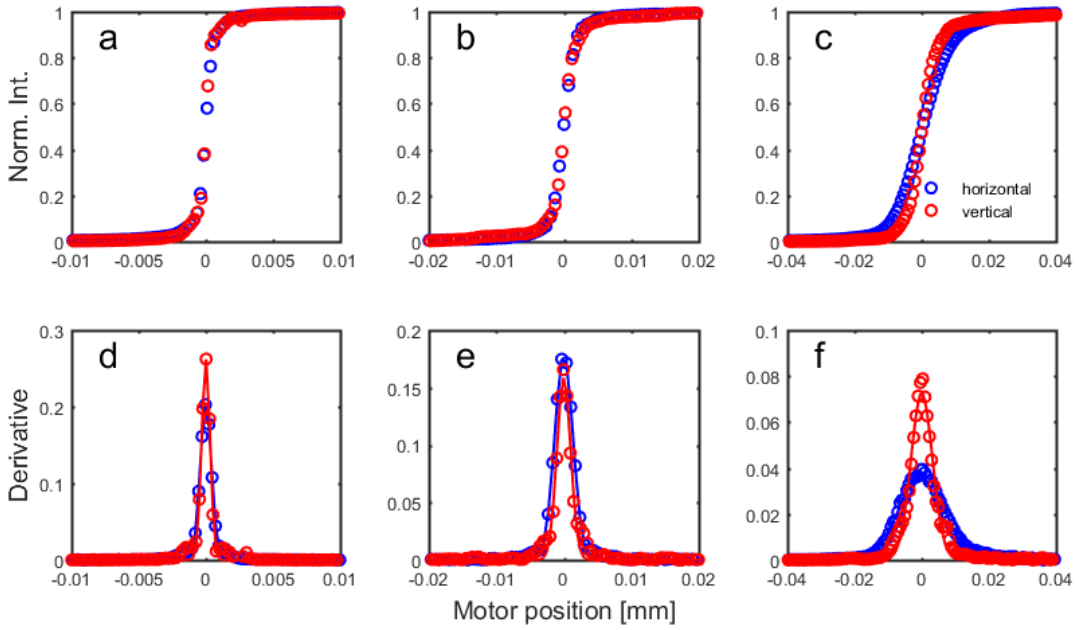

Figure 2: (a) Knife-edge scans and (d) derivatives of the short focus option, (b) knife-edge scans and (e) derivatives of the transfocator option and (c) knife-edge scans and (e) derivatives of the medium focus option. The red color displays scans in the vertical, the blue color displays scans in the horizontal direction, solid lines are model fits using a Gaussian function. All data sets were recorded at 8.8 keV.

(horizontal) focal spot size changes as a function of the vertical (horizontal) beam defining slit size, while the influence of the size of the beam defining aperture perpendicular to this direction is negligible.

As the geometrical acceptance of the CRL-stack installed for this photon energy is greater than the probed illumination size of the beam, the focal spot size decreases both in the vertical and in the horizontal direction for increasing beam defining slit sizes in the respective direction. The smallest focal spot size is therefore measured for the largest beam defining slit aperture used during the measurement. Please note that this option allows to enhance the photon flux on the sample considerably - while the number of photons collected by the lenses increases with increasing illumination defining aperture, the beam-size at the sample position decreases.

3 Conclusion

If one studies statistical properties of a disordered sample system, it is advantageous to match the speckle size to the pixel size of the detector. One possibility is to vary the beam-size on the sample, an option that is experimentally relatively easily accessible. We have shown how compound refractive lenses placed at different distances from the sample position can be used to achieve different beam-sizes on the sample, thus allowing to tailor the speckle visibility and the radiation dose depending on the investigated sample system. The obtained focal spot sizes are in good agreement with theoretical values. For even smaller focal sizes than currently available at the multi-purpose XPCS setup of beamline P10, the influence of lens abberations on the obtainable focal spot site start to play a prominent role, making the use of corrective phase plates for the correction of the lens stack desirable [13]. In addition to changing the focal spot size on the sample, the three different focussing possibilities allow to change the flux density and thus the dose impinging on the sample. The focal spots measured at 8.8 keV are 0.7 μm^2 for the SF, 7.7 μm^2 for the TF and 118.6 μm^2 for the MF. Assuming an identical photon flux in front of the CRLs, and taking into account the different transmissions of the respective lens stacks (0.92 for the SF, 0.96 for the TF and 0.97 for the MF), this allows to vary the dose on the sample by more than a factor of 100 for experiments with radiation sensitive samples and not demanding speckle visibility requirements.

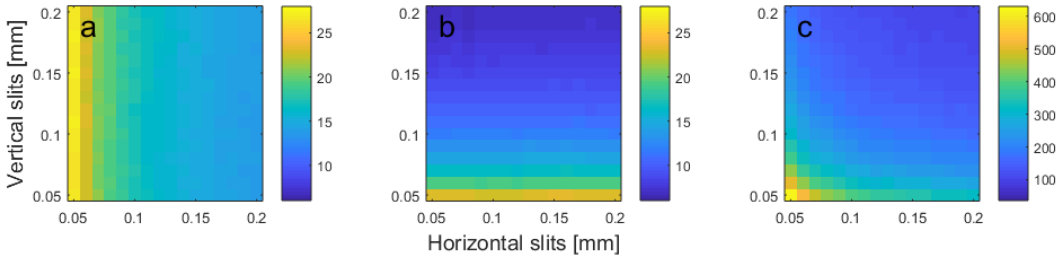

Figure 3: (a) 2d map of the horizontal beam-size, (b) 2d map of the vertical beam-size and (c) the resulting beam-area as a function of beam defining aperture in the vertical and horizontal direction. The unit of the colorbar is μm for (a) and (b) and μm^2 for (c). The data have been taken at 8.8 keV using the medium focus option.

4 Acknowledgments

We would like to thank all PETRA III support teams for their continuous help during the operation of beamline P10. We acknowledge DESY (Hamburg, Germany), a member of the Helmholtz Association HGF, for the provision of experimental facilities. This work was carried out at beamline P10 of PETRA III.

References

[1] Snigirev, A and Kohn, V and Snigireva, T and Lengeler, B 1996 *Nature* **384** 49-51

[2] Lengeler, B and Schroer, CG and Tümmler, J and Benner, B. and Richwin, M and Snigirev, A and Snigireva, I and Drakopoulos, M 1999 *J. Synchrotron Rad* **6** 1153–1167

[3] Grübel, G and Zontone, F 2004 *J. Alloys* **362** 3–11

[4] Sutton, MA 2008 *C. R. Phys.* **9** 657–67

[5] Robinson, IK and Vartanyants, IA and Williams, GJ and Pfeifer, MA and Pitney, JA 2001 *Phys. Rev. Lett.* **87** 195505

[6] Miao, J and Sayre D and Chapman HN 1998 *J. Opt. Soc. Amer.* A **15** 1662–69

[7] Giewekemeyer, K and Neubauer, H and Kalbfleisch, S and Krüger, SP and Salditt T 2010 *New J. Phys* **12** 035008

[8] Kalbfleisch, S and Osterhoff, M and Giewekemeyer, K and Neubauer, H and Krüger, SP and Hartmann, B and Bartels, M and Sprung, M and Leupold, O and Siewert, F and Salditt T 2010 *AIP. Conf. Proc.* **1234** 433–6

[9] Zozulya, AV and Bondarenko, S and Schavkan, A and Westermeier, F and Grübel, G and Sprung, M 2012 *Opt. Express* **20** 18967

[10] Lengeler, B and Schroer, CG and Benner, B and and Gerhardus, A and Günzler, TF and Kuhlmann, M and Meyer, J and Zimprich, C 2002 *J. Synchrotron Rad* **9** 119–124

[11] Singer, A and Vartanyants, IA 2014 *J. Synchrotron Rad* **21** 5–15

[12] Kohn, VG 2017 *J. Synchrotron Rad* 609–614

[13] Seiboth, F and Schropp, A and Scholz, M and Wittwer, F and Rödel, C and Wünsche, M and Ullsperger, T and Nolte, S and Rahomäki, J and Parfeniukas, K and Giakoumidis, S and Vogt, U and Wagner, U and Rau, C and Boesenberg, U and Garrevoet, J and Falkenberg, G and Galtier, EC and Ja Lee, H and Nagler, B and Schroer, CG 2017 *Nat. Communications* **8** 14623